



Berg Huettenmaenn Monatsh (2023) Vol. 168 (1): 15–19  
<https://doi.org/10.1007/s00501-022-01314-3>  
 © The Author(s) 2023

**BHM** Berg- und  
 Hüttenmännische  
 Monatshefte

## (In Situ) Determination of Hydrogen Entry into Galvanized Dual-phase Steel During Corrosive Exposure

Gabriela Schimo-Aichhorn<sup>1</sup>, Ines Traxler<sup>1</sup>, Andreas Muhr<sup>2</sup>, Gerald Luckeneder<sup>2</sup>, Josef Faderl<sup>2</sup>, Sandra Grienberger<sup>2</sup>, Hubert Duchaczek<sup>2</sup>, Karl-Heinz Stellnberger<sup>2</sup>, Darya Rudomilova<sup>3</sup>, Tomas Prosek<sup>3</sup>, David Stifter<sup>4</sup>, and Sabine Hild<sup>4</sup>

<sup>1</sup>CEST Competence Centre for Electrochemistry and Surface Technology, Linz, Austria

<sup>2</sup>voestalpine Stahl, Linz, Austria

<sup>3</sup>Technopark Kralupy, University of Chemistry and Technology Prague, Prague, Czech Republic

<sup>4</sup>ZONA Zentrum für Oberflächen- und Nananalytik, Johannes Kepler University Linz, Linz, Austria

Received October 15, 2022; accepted November 23, 2022; published online January 18, 2023

**Abstract:** The aim of this contribution is to present a comprehensive approach to study the extent of hydrogen entry into a hot-dip-galvanized DP1000 steel, which is exposed to corrosive conditions. For this purpose, the Z100 coating was immersed in 5% sodium chloride solution at room temperature. The distribution of hydrogen and the spots of increased hydrogen entry were detected with scanning Kelvin probe (SKP) and scanning Kelvin probe force microscopy (SKPFM). Effects of hydrogen inserted during corrosion on the mechanical properties were determined in slow-strain rate tests (SSRT). Hydrogen quantification was achieved via thermal desorption mass spectrometry (TDMS), giving additional insights into the mobility of the inserted hydrogen within the steel by distinguishing diffusible and trapped hydrogen.

**Keywords:** Hydrogen embrittlement, Corrosion, Zn-based coatings, Dual-phase steel, Hydrogen analysis

**(In situ) Bestimmung des Wasserstoffeintrages in galvanisierten Dualphasenstahl unter korrosiven Bedingungen**

**Zusammenfassung:** Das Ziel dieses Beitrags ist die methodenübergreifende Analyse des Wasserstoffeintrages in feuerverzinkten Dualphasenstahl (DP1000) unter korrosiven Bedingungen. Dazu wurde die Z100 Beschichtung der Proben einer Korrosion durch Immersion in 5% Natriumchloridlösung bei Raumtemperatur ausgesetzt. Die resultierende Wasserstoffverteilung in der Probe sowie

Bereiche mit erhöhtem Wasserstoffeintrag konnten mittels Rasterkelvinsonde und Rasterkraft-Kelvinsondenmikroskopie detektiert werden. Die Auswirkung des Wasserstoffs auf die mechanischen Eigenschaften wurde in Langsamzugversuchen analysiert. Die Quantifizierung des eingetragenen Wasserstoffs erfolgte mittels Thermischer Desorptions-Massenspektrometrie, die zusätzlich Einblicke in die Beweglichkeit des Wasserstoffs im Metallgitter ermöglichte, indem zwischen frei beweglichem Wasserstoff und Wasserstoff, immobilisiert in Fallen, unterschieden werden konnte.

**Schlüsselwörter:** Wasserstoffversprödung, Korrosion, Zink-basierte Beschichtungen, Dualphasenstahl, Wasserstoffbestimmung

### 1. Introduction

The analysis of hydrogen entering steel structures and components under corrosive conditions is an essential element to assess the risk of hydrogen embrittlement related failure of steel in service life, e.g. in the automotive industry [1]. Even though hydrogen detection is a highly complex task, several techniques were developed to characterize the hydrogen amount, its distribution, and its impact on mechanical properties, especially of materials that are prone to hydrogen embrittlement such as advanced high strength steels [2].

The present contribution utilizes localized and global hydrogen detection techniques as well as mechanical tests to study the corrosive hydrogen entry using the example of galvanized DP1000 corroding in sodium chloride solution.

Assoz. Prof. DI Dr. D. Stifter (✉)  
 ZONA Zentrum für Oberflächen- und Nananalytik,  
 Johannes Kepler University Linz,  
 Altenberger Str. 69,  
 4040 Linz, Austria  
 David.stifter@jku.at

TABLE 1  
Composition of DP1000 steel according to EN 10346

Grade	C <sub>max</sub> %	Si <sub>max</sub> %	Mn <sub>max</sub> %	P <sub>max</sub> %	S <sub>max</sub> %	Al <sub>total</sub> %	Cr + Mo <sub>max</sub> %	Ti + Nb <sub>max</sub> %	V <sub>max</sub> %	B <sub>max</sub> %
HCT980X	0.2	1	2.5	0.08	0.015	0.015–2.0	1.4	0.15	0.2	0.005

## 2. Experimental Procedure

A hot-dip galvanized dual-phase steel (DP1000) with the composition shown in Table 1, was investigated. The average thickness of the Z100 coating was approximately 7  $\mu\text{m}$ , while the thickness of the samples was 1.2 mm. The hydrogen diffusion coefficient of the investigated steel grade was determined to  $1.5 \times 10^{-6} \text{ cm}^2 \text{ s}^{-1}$  in a previous work [3].

SKP measurements were performed with an instrument from Wicinski-Wicinski GbR using a 180  $\mu\text{m}$  diameter Cr-Ni tip and a tip-sample distance of 15  $\mu\text{m}$  to scan the surface. The atmosphere in the sample compartment of the instrument was kept at 40% relative humidity and 25 °C throughout the experiments. To enable correlation of the measured contact potential difference (CPD) with electrochemical potentials, the tip was calibrated prior to the measurement against a copper/saturated copper sulphate solution. The SKP scan side of the sample was pickled with inhibited, 1:1 diluted hydrochloric acid solution (including 4.5 g l<sup>-1</sup> hexamethylenetetramine) to remove the Zn coating, while the hydrogen entry side was treated with an engraving instrument to introduce a 5 mm long and 200  $\mu\text{m}$  broad line defect. For the SKP measurements the coated sample side with the line defect was brought in contact with a hydrogel corrosion patch carrying 5% NaCl solution. Further details of the experimental procedure are described elsewhere [4].

A detailed procedure of sample preparation and measurement parameters for SKPFM experiments are described elsewhere [5]. In order to induce corrosion at the hydrogen entry side, a 10  $\mu\text{l}$  droplet of 1M NaCl solution was applied prior to the measurement start. Changes in potential or CPD, respectively, were then recorded by a continuous scanning of the prepared steel surface on the hydrogen exit side.

Slow-strain rate tests were conducted with a tensile testing machine (ZwickRoell) with a strain rate of  $1.10^{-6} \text{ s}^{-1}$ . A corrosion cell was attached to the middle part of the sample and, for some of the samples, filled with 5% NaCl solution. The samples, produced by milling, had a total length of 250 mm, a parallel length of 120 mm and were 20 mm broad.

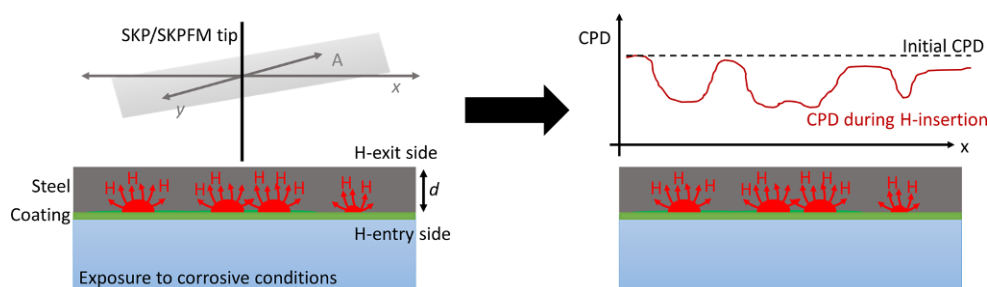
Hydrogen quantification was performed via thermal desorption mass spectrometry (TDMS) with a Bruker Galileo G8 with an IR furnace, coupled to a GAM200 mass spectrometer from InProcess Instruments. Samples with a size of  $55 \times 20 \text{ mm}^2$  were heated up to 900 °C with a heating rate of  $20 \text{ K min}^{-1}$ . Prior to the measurements, the zinc coating was removed by pickling in inhibited HCl, as described above.

## 3. Results and Discussion

Among the available methods for localized hydrogen detection in metals, SKP and SKPFM are especially useful tools for iron and steel samples. As iron oxide layers interact with hydrogen ( $\text{Fe}^{3+}$  is reduced to  $\text{Fe}^{2+}$  [6]), the local hydrogen concentration is reflected by a decrease in contact potential difference (CPD), measured with SKP and SKPFM (Fig. 1). Usually, the hydrogen is originating from the interior of the samples and/or from the reverse sample side, where it is introduced either by cathodic polarization or corrosion. Both techniques are non-destructive and can be applied in atmosphere without the need of applying electrolyte solution as in standard electrochemical methods. Stable conditions at the scanned sample side are essential to guarantee that observed potential changes are solely caused by hydrogen. Using SKP, larger areas of several  $\text{cm}^2$  can be scanned in a reasonable time frame. Therefore, it can be used to detect regions with increased hydrogen entry rates, e.g. at defects in protective coatings on steel (Fig. 2).

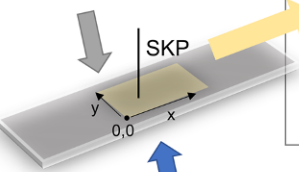
Compared to SKP, the AFM-based SKPFM-technique offers a much higher spatial resolution: utilizing an AFM cantilever with a tip size of several nm, coated with a conductive layer, both the topography and the CPD can be mapped of areas in the range of ca.  $100 \mu\text{m}^2$ . This makes it an ideal tool to study hydrogen related CPD changes within the microstructure. For this purpose, samples have to be prepared carefully by etching and electropolishing in order to reveal the microstructure without introducing too pronounced features, such as steps, on the surface that could lead to measurement artefacts. The individual grains and phases can be distinguished in the topography image,

Fig. 1: Schematic of SKP and SKPFM measurements to monitor hydrogen, which is entering a steel sample under corrosive conditions and permeating towards the exit side, via changes in the contact potential difference (CPD)



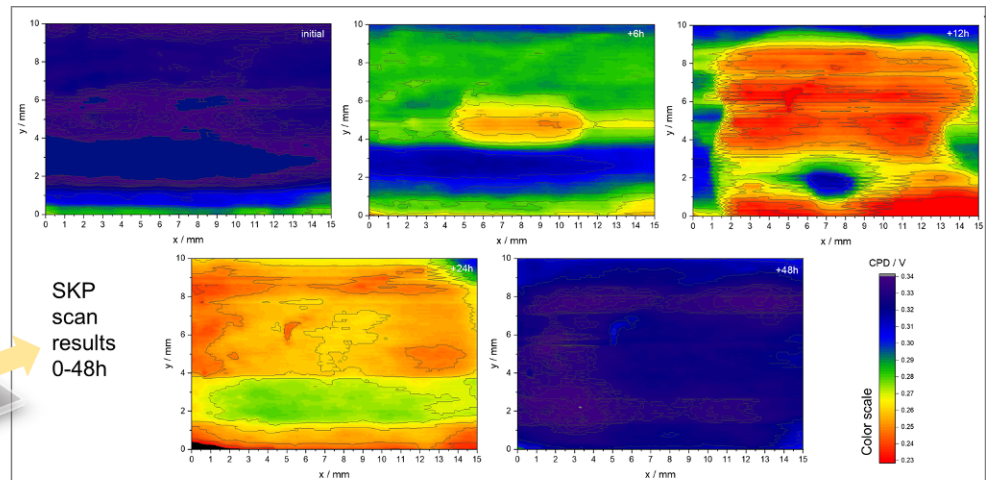
Visualisation of permeating hydrogen, inserted at H-entry side due to corrosion

steel surface (H-exit side)



Corroding Zn coated steel (H-entry side)

Artificial defect in Zn-coating



SKP scan results 0-48h

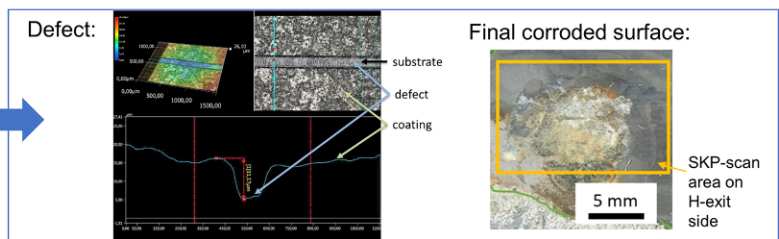
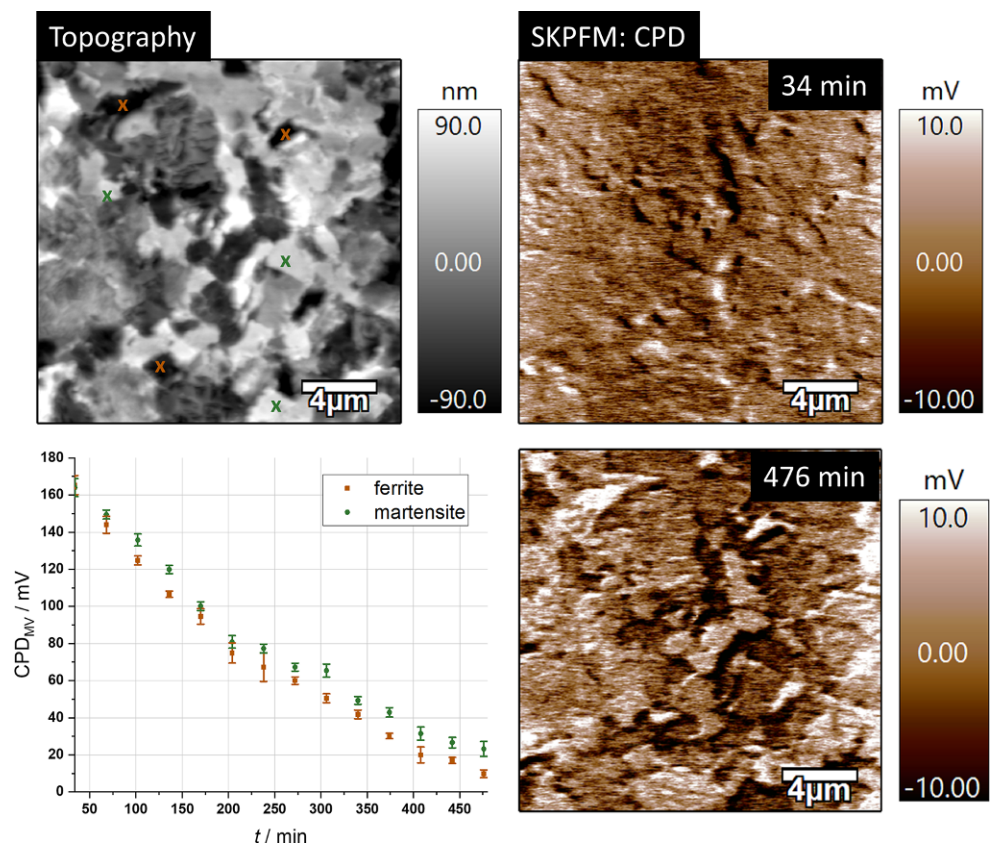


Fig. 2: SKP surfacescans ( $15 \times 10 \text{ mm}^2$ ) on the uncoated, uncorroded steel surface from initial state to 48 h after start of corrosion of the Z-coated hydrogen entry side, where an artificial line defect was engraved to expose the steel surface

Fig. 3: SKPFM scan results measured on the hydrogen exit side (zinc coating removed, electropolished) of a DP1000 sample. Changes of average CPD and relative CPD values due to permeating hydrogen, inserted into the Z-coated side of the sample due to corrosive processes



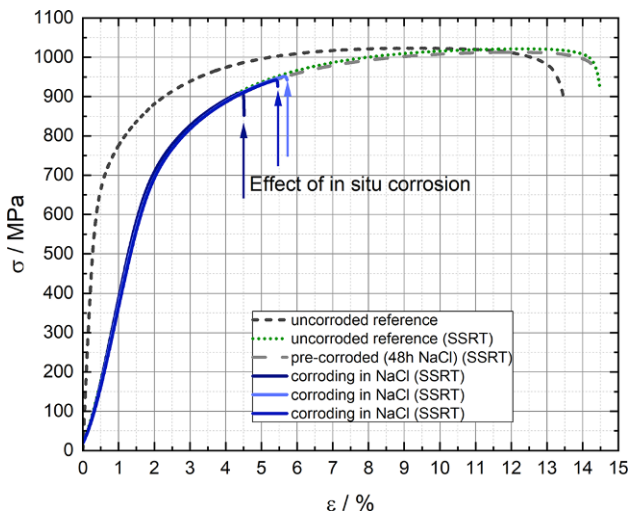


Fig. 4: Results of slow-strain rate tests (SSRT) performed on Z100 coated DP1000 under immersion in 5% NaCl in comparison to results of an uncorroded reference sample and a pre-corroded sample, which was immersed into 5% NaCl 48 h prior to the SSRT. As no extensometer is used in SSRT with corrosion cell attached, the stress-strain curve recorded with extensometer is added

while changes in the SKPFM-scan result can be due to permeating hydrogen. In case of the experiment, depicted in Fig. 3, hydrogen was inserted on the Z-coated sample side due to corrosion after application of a 10  $\mu$ l droplet of 1 M NaCl solution. For comparison of CPD changes of the ferrite and martensite phases, the average CPD of 3 grains each were plotted over time. A slightly larger and faster decline of potential could be observed for ferritic grains, which could be due to higher diffusion rates in ferrite. However, the difference between the hydrogen induced changes between the phases is small as the sequence of grains/phases in the interior of the sample, which hydrogen has to pass before it arrives at the exit side, might have a homogenizing effect.

Slow-strain rate tests are, in many cases, the method of choice for determining the effect of hydrogen on the me-

chanical properties of a steel sample. In this contribution, tensile test specimens were corroded in situ by immersing the sample in 5% NaCl while straining. Compared to a non-corroded reference as well as a sample, which was corroded prior to tensile testing by immersion in 5% NaCl for 48 h, a difference in elongation can be observed (from 13.49% to average 5.24%) for in situ corroding samples, while the tensile strength is only subtly reduced (from 1026 to 938 MPa). The difference in results between in situ and pre-corroded samples suggest that the detrimental effect of hydrogen is maximized when its presence is directly coupled to the application of stress and that the corrosive entry of hydrogen is a highly reversible process (Fig. 4).

Regarding the SSRT results it is important to determine the hydrogen concentration in the sample before fracture occurs. Therefore, in another SSRT experiment under corrosive conditions, the tensile test was stopped at an elongation of 4%. The sample was dried and immediately stored in liquid nitrogen until its preparation for TDMS measurement. Compared to a non-corroded reference, the thermal desorption spectrum of the corroded and strained sample shows increased amounts of diffusible hydrogen (+0.047 ppm), which is visible in a temperature range between 50 and 250  $^{\circ}$ C, but also increased amounts of trapped hydrogen above 350  $^{\circ}$ C (0.289 ppm vs. 0.121 ppm). Trapped hydrogen in the reference sample has its origin in the production process, while the diffusible hydrogen is exclusively introduced in this case due to corrosive degradation processes occurring on the sample surface and can be seen as main cause for the change in elongation (Fig. 5).

#### 4. Conclusions

The present contribution shows the inevitable need of combining different methods for the investigation of hydrogen embrittlement related material degradation and for obtaining deeper insights into hydrogen-material interactions. For corrosive hydrogen entry, SKP measurements can indicate the locations where hydrogen entry is favor-

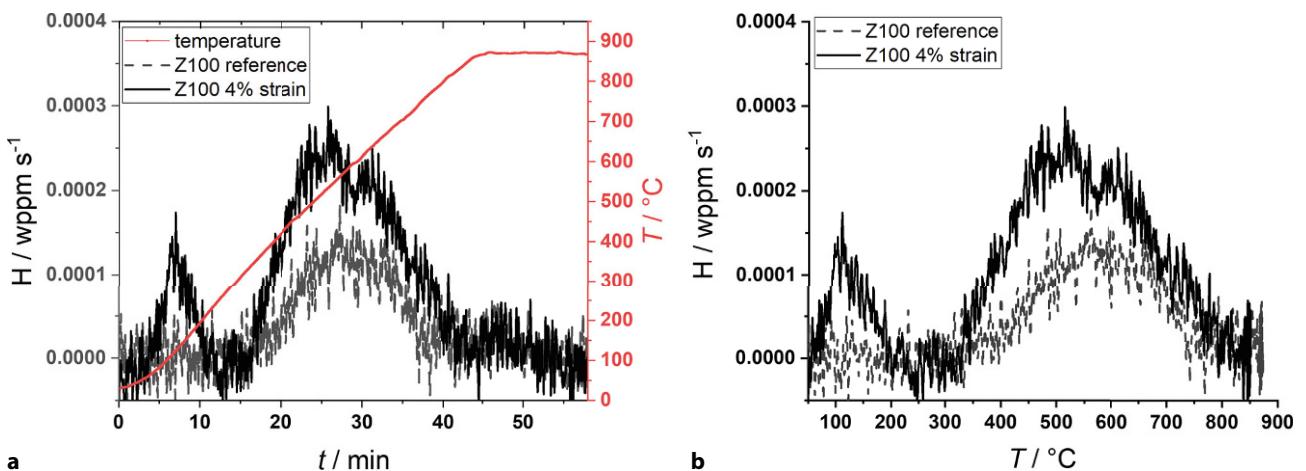


Fig. 5: Hydrogen thermal desorption spectra of DP1000-Z100 after straining to 4% elongation during immersion in 5% NaCl in comparison with a non-corroded, non-strained reference sample: **a** H mass flux and temperature versus time, **b** H mass flux versus temperature

able and the evolution of hydrogen entry over time. SKPFM gives additional insights into diffusion pathways within the microstructure. Deteriorative effects of hydrogen have to be clarified in mechanical tests, such as slow-strain rate tests, complemented by hydrogen quantification measurements in order to establish a connection between hydrogen concentration and mechanical behavior.

All of the described experiments and methods are frequently conducted under relatively harsh conditions to reveal the sample performance in the worst case and might not reflect the reality in detail. However, this approach can serve as a basis for assessing the risk of a hydrogen embrittlement related failure of a material in service.

**Acknowledgements.** The Comet Centre CEST is funded within the framework of COMET—Competence Centers for Excellent Technologies by BMVIT, BMDW as well as the Province of Lower Austria and Upper Austria. The COMET programme is run by FFG. This work originates from research in H-Hunt II (FFG 865864 CEST-K1, since 2019) project. The authors gratefully thank voestalpine Stahl GmbH for the support.

**Funding.** Open access funding provided by Johannes Kepler University Linz.

**Open Access** This article is licensed under a Creative Commons Attribution 4.0 International License, which permits use, sharing, adaptation, distribution and reproduction in any medium or format, as long as you give appropriate credit to the original author(s) and the source, provide a link to the Creative Commons licence, and indicate if changes were made. The images or other third party material in this article are included in the article's Creative Commons licence, unless indicated otherwise in a credit line to the material. If material is not included in the article's Creative Commons licence and your intended use is not permitted by statutory regulation or exceeds the permitted use, you will need to obtain permission directly from the copyright holder. To view a copy of this licence, visit <http://creativecommons.org/licenses/by/4.0/>.

## References

1. Scharf, R., Muhr, A., Luckeneder, G., Larour, P., Mraczek, K., Rehrl, J., Leomann, F., Stellnberger, K.-H., Faderl, J., Mori, G.: Hydrogen embrittlement of DP-1000 flat steel sheet: Influence of mechanical properties, specimen geometry, pre-damaging and electrolytically zinc galvanizing. *Mater. Corros.* **67**(3), 239–250 (2016)
2. Rudomilova, D., Prosek, T., Luckeneder, G.: Techniques for investigation of hydrogen embrittlement of advanced high strength steels. *Corros. Rev.* **36**(5), 413–434 (2018)
3. Rudomilova, D., Prosek, T., Salvetr, P., Knaislova, A., Novak, P., Kodym, R., Schimo-Aichhorn, G., Muhr, A., Duchaczek, H., Luckeneder, G.: The effect of microstructure on hydrogen permeability of high strength steels. *Mater. Corros.* **71**(6), 909–917 (2020)
4. Schimo-Aichhorn, G., Traxler, I., Muhr, A., Luckeneder, G., Duchaczek, H., Stellnberger, K.-H., Faderl, J., Rudomilova, D., Prosek, T., Stifter, D., Hild, S.: Investigations on corrosion behaviour and hydrogen embrittlement susceptibility of galvanized dual-phase steel. In: *Galvatech 2021—ASMET—12th international conference on Zinc & Zinc alloy coated steel sheet Proceedings Vienna*. pp. 1004–1013. (2021)
5. Traxler, I., Schimo-Aichhorn, G., Muhr, A., Commenda, C., Jerrar, A., Sagl, R., Mraczek, K., Rudomilova, D., Luckeneder, G., Duchaczek, H., Stellnberger, K.-H., Prosek, T., Hassel, A.W., Hild, S.: Optimization of metallographic sample preparation for AFM/SKPFM based phase distinction of complex and dual phase high strength steels. *Pract. Metallogr.* **58**(6), 308–331 (2021)
6. Williams, G., McMurray, H.N., Newman, R.C.: Surface oxide reduction by hydrogen permeation through iron foil detected using a scanning Kelvin probe. *Electrochem. commun* **27**, 144–147 (2013)

**Publisher's Note.** Springer Nature remains neutral with regard to jurisdictional claims in published maps and institutional affiliations.